

High-resolution structure of $\text{Zn}_3(\text{HOTP})_2$ (HOTP = hexaoxidotriphenylene), a three-dimensional conductive MOF

Kimberly J. Zhang, Tianyang Chen, Julius Oppenheim, Luming Yang, Lukáš Palatinus, Peter Müller, Troy Van Voorhis, Mircea Dincă*

Table of Contents

1. Materials and General Information	2
2. Synthetic Procedures	4
3. PXRD Comparison of $\text{Zn}_3(\text{HOTP})_2$ Synthesized Under Different Conditions	5
4. N_2 Adsorption Isotherm	6
5. Thermogravimetric Analysis (TGA).....	7
6. UV-Vis Spectra.....	8
7. Crystallographic Table	10
8. Reciprocal Space Sections	11
9. DFT Optimized Structure.....	17
10. Room Temperature Conductivity Measurements.....	21
11. References.....	22

1. Materials and General Information

All of the chemicals including Zn(OAc)₂· 2H₂O, 2,3,6,7,10,11-hexahydroxytriphenylene (H₆HOTP), and dimethylformamide (DMF) were purchased through Sigma-Aldrich or TCL and used without further purification.

Methods

Computation was performed using FHI-AIMS with periodic boundary conditions. Geometry optimization was carried out using the 3-fold approximate structure with disorder removed resolved by electron diffraction¹. The generalized gradient approximation function parametrized by Perdew-Burke-Ernzerhof was used to describe the exchange-correlation potential and the total energy was converged to within 10⁻⁵ eV². Subsequent calculations including band structure calculations and projected density of states were performed using the optimized structure. Hybrid function HSE06 was used to describe the more accurate exchange-correlation potential³. A Γ -centered k-point mesh of 3×3×4 was used for the Brillouin integrations⁴.

3D ED data were collected and processed using the following procedure: The sample was very gently ground in an agate mortar. A TEM copper grid with holey carbon film was slid on the sample to stick some of the crystals onto the grid, and the excess was tapped off. The grid was loaded onto a sample holder and inserted into FEI Tecnai G2 20 TEM. The microscope was operated at 200 kV, and data were recorded on a Medipix 3 hybrid pixel detector ASI Cheetah (512x512 pixels, 24bit dynamic range). The tilt step per frame was 0.3°, with the exposure time of 799 ms per frame.

Indexing, lattice parameter determination, and peak integration were performed using PETSc⁵. The processed data were imported into Jana2020⁶, and the crystal structure was solved in superspace using Superflip^{7,8}. The structure was refined using the superspace formalism.

Laboratory powder X-ray diffraction (PXRD) patterns were recorded using a Bruker Advance II diffractometer equipped with a $\theta/2\theta$ reflection geometry and Ni-filtered Cu K α radiation ($K\alpha_1 = 1.5406 \text{ \AA}$, $K\alpha_2 = 1.5444 \text{ \AA}$, $K\alpha_2/K\alpha_1 = 0.5$). The tube voltage and current were 40 kV and 40 mA, respectively. Samples for PXRD were prepared by placing a thin layer of the appropriate material on a zero-background silicon crystal plate.

N₂ adsorption isotherms were measured by a volumetric method using a Micromeritics ASAP 2020 Plus gas sorption analyzer. An oven-dried sample tube equipped with a TranSealTM (Micromeritics) was evacuated and tared. The sample was transferred to the sample tube, which was then capped with a TranSeal. The sample was activated at 90 °C under high dynamic vacuum (< 10⁻⁴ mbar) for 24 hours before analysis. The N₂ isotherm was measured using a liquid nitrogen bath at 77 K. Ultrahigh purity grade (99.999% purity) N₂, oil-free valves and gas regulators were used for all the free space correction and measurements. Fits to the BrunauerEmmett-Teller (BET) equation satisfied the published consistency criteria. The pore size is calculated by the Zeo++ software.

Pore diameters were calculated using the Zeo++ software with command “./zeo++-0.3/network -ha -res file.cif”

Thermogravimetric analysis (TGA) was performed on a TA Instruments Q500 Thermogravimetric Analyzer at a heating rate of 2.0 °C/min under dry air gas flow of 5 mL/min on a platinum pan from room temperature to 600 °C.

Scanning electron microscopy (SEM) was conducted at MIT MRSEC (formerly the Center for Materials Science and Engineering, or CMSE) on a Zeiss Merlin high-resolution scanning electron microscope with an InLens detector at an operating voltage of 3 or 4 kV.

Room temperature conductivity measurements was conducted via two-contact probe measurements were carried out at 296 K in ambient atmosphere on pressed pellets using a home-built two-probe *in situ* press set-up described previously. Linear I–V curves were obtained by sweeping the voltage between –1 and +1 V and measuring the current using a sourcemeter (Keithley 2450) connected to the press via test leads (Keithley 8608). Pellet thicknesses were measured after the measurement using a micrometer (Mitutoyo).

Elemental analyses were carried out by Robertson Microlit Laboratories in Ledgewood, New Jersey.

2. Synthetic Procedures

Synthesis of Zn₃HOTP₂ (Zn₃C₃₆O₁₂H₁₂). Zn(OAc)₂ · 2H₂O (24.6 mg, 0.112 mmol, 1.82 eq.) was dissolved in 4.4 mL of DI water in a 20 mL glass vial and sonicated for 5 min. In a separate vial, H₆HOTP (20 mg, 0.0617 mmol, 1 eq.) was dissolved in 1.28 mL *N,N*-dimethylformamide (DMF) and sonicated for 5 min. The solution containing H₆HOTP was filtered through a 0.22 µm PTFE syringe filter and added to the Zn salt solution. The mixture was heated at 85 °C for 8 hr. Afterwards, the mixture was cooled to room temperature, and washed with water (5 mL, 3 times), ethanol (5 mL, 3 times), and acetone (5 mL, 3 times). 8.92 mg (0.0214 mmol per HOTP, 35% yield) of a black powder were recovered. The measured elemental composition (meas, C: 43.27%, H: 3.36%, N: 0.87%) matches well with a hydrated formula Zn₃HOTP₂·9.73H₂O·0.65DMF (calc, C: 44.07%, H: 3.10%, N: 0.84%).



3. PXRD Comparison of $\text{Zn}_3(\text{HOTP})_2$ Synthesized Under Different Conditions

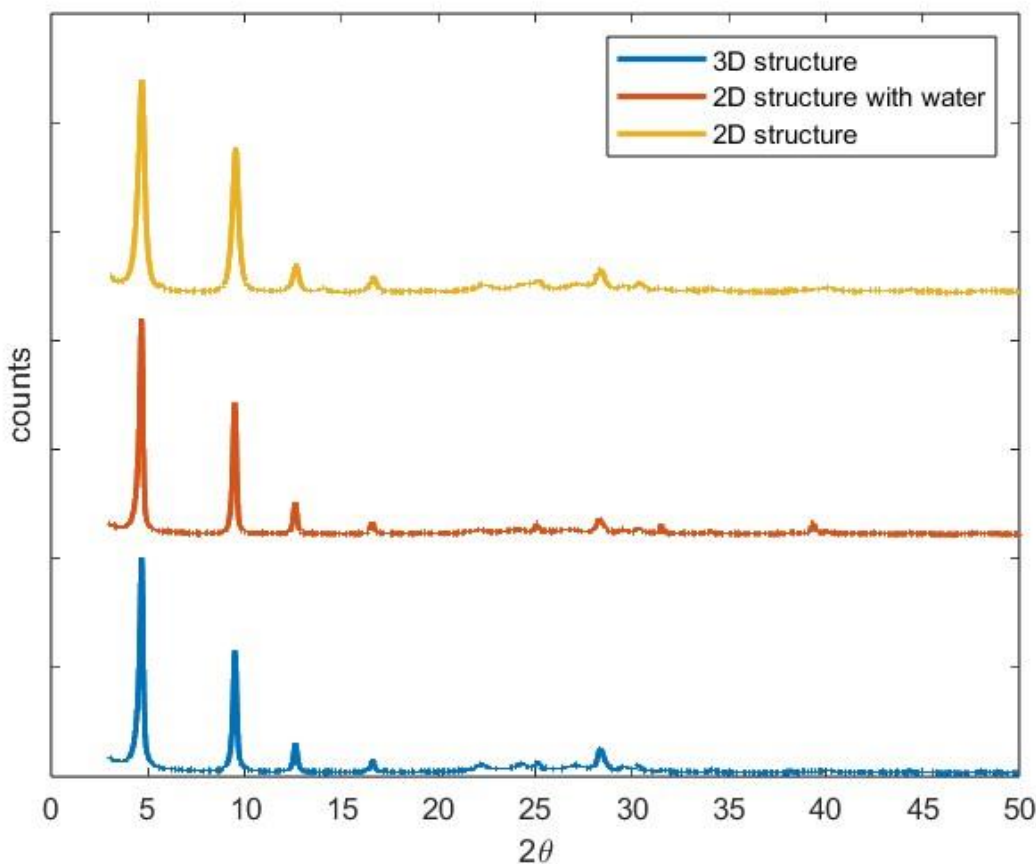


Figure S1. PXRD traces of $\text{Zn}_3(\text{HOTP})_2$ synthesized via three distinct procedures: our reported 3D framework (blue), a literature method reported to yield a 2D structure with Zn^{2+} adopting octahedral geometry,¹⁰ and a second method reported to give a 2D structure with Zn^{2+} adopting square-planar geometry (yellow).⁹ All three samples exhibit nearly identical diffraction patterns, including the low-angle features often attributed to 2D layer stacking. These results underscore that PXRD alone is insufficient to unambiguously distinguish between topologically 2D and 3D phases in this system. High-resolution structural techniques (e.g., 3D electron diffraction) are necessary to resolve the actual framework connectivity and dimensionality.

4. N₂ adsorption isotherm

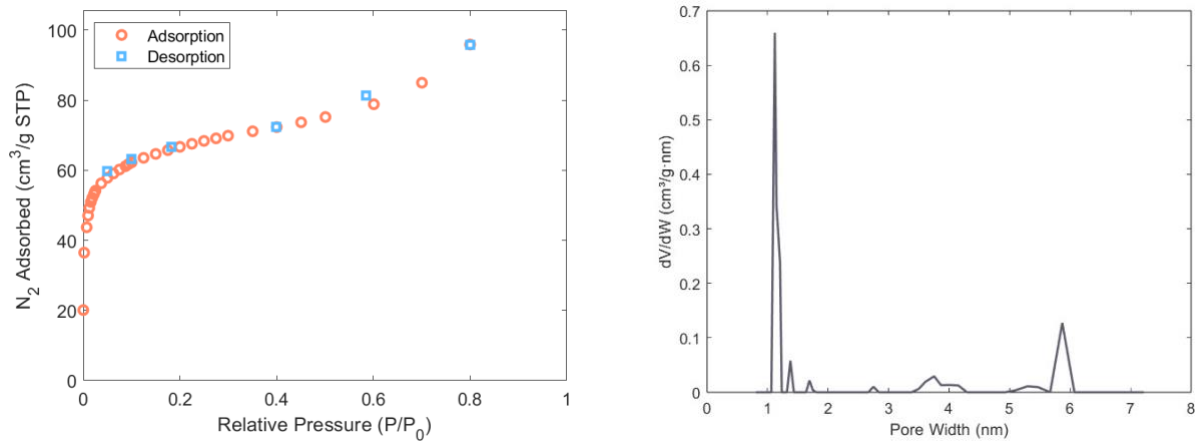


Figure S2. Nitrogen adsorption and desorption experiments of Zn₃(HOTP)₂ at 77 K. Left: Nitrogen adsorption (red circles) and desorption (blue squares) isotherms measured at 77 K for activated Zn₃(HOTP)₂. The isotherm exhibits Type I behavior with a slight hysteresis loop, indicative of microporosity with some mesoporous contributions. Right: Pore size distribution calculated from the desorption branch using the BJH method, showing a sharp peak centered around \sim 1.1 nm with minor mesopore contributions near \sim 6 nm. The calculated pore size using the crystal structure is 14 Å. We note that the slightly smaller experimental pore size could result from the incomplete removal of guest water molecules since the material was activated at 90 °C, and/or the limitation of the BJH model.

5. Thermogravimetric analysis (TGA)

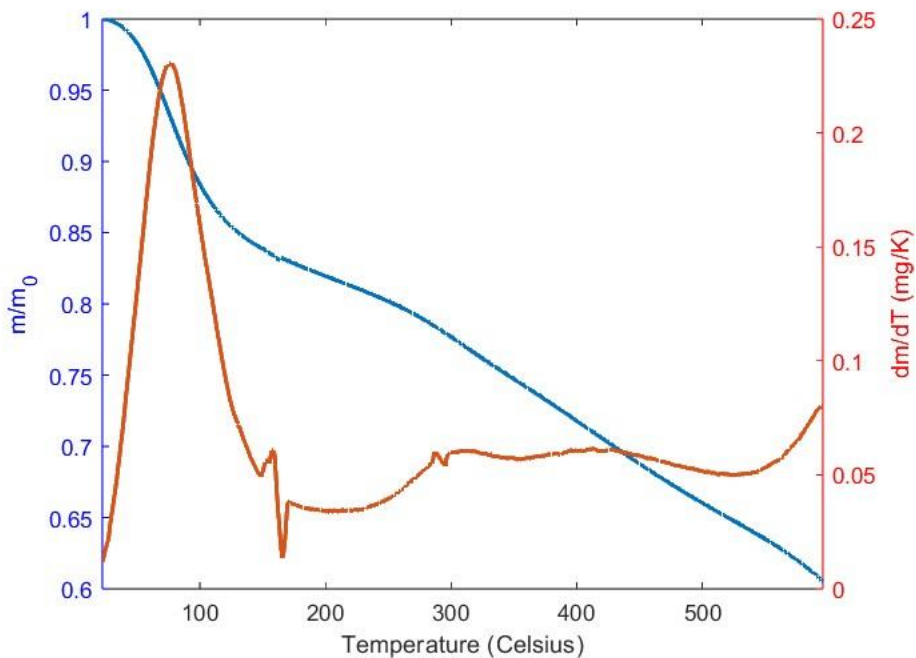


Figure S3. TGA trace of $\text{Zn}_3(\text{HOTP})_2$ at 77 K. Blue: remaining relative mass; red: derivative of the weight change. The initial mass loss ($\sim 7\text{--}10\%$) occurring below 150 °C corresponds to the desorption of guest water and residual solvent molecules, consistent with elemental analysis and the hydrophilic nature of the framework. The gradual mass loss from $\sim 150\text{--}500$ °C is attributed to partial framework decomposition. The profile supports the presence of pore-adsorbed water in the as-synthesized sample and validates the need for thermal activation prior to sorption measurements or electron diffraction.

6. UV-Vis Spectra

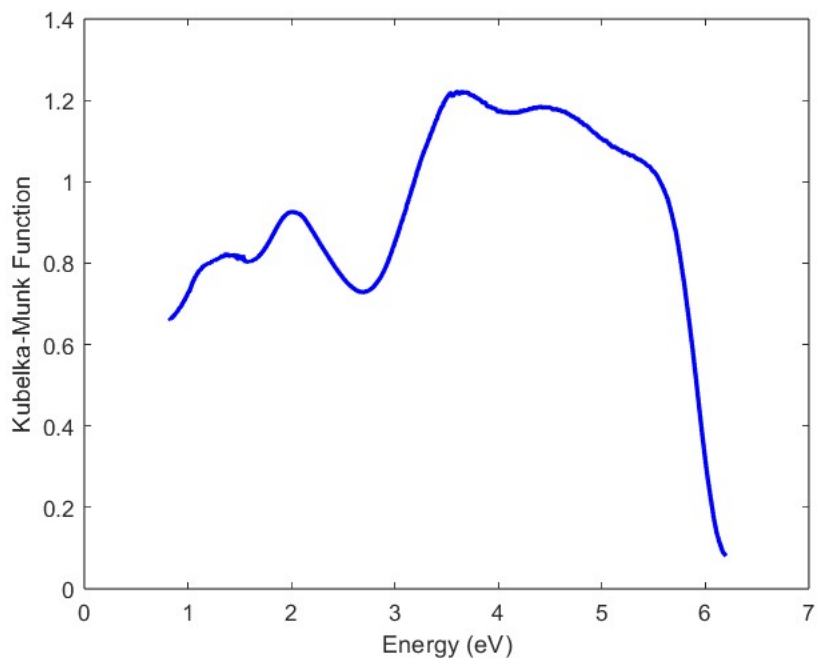


Figure S4. UV-Vis spectra (plotted as Kubelka Munk transform) of $\text{Zn}_3(\text{HOTP})_2$. Multiple absorption features are observed across the visible range, consistent with $\pi-\pi^*$ transitions localized on the HOTP ligands. The strong absorption onset near ~ 1.5 eV suggests an optical gap consistent with semiconducting behavior.

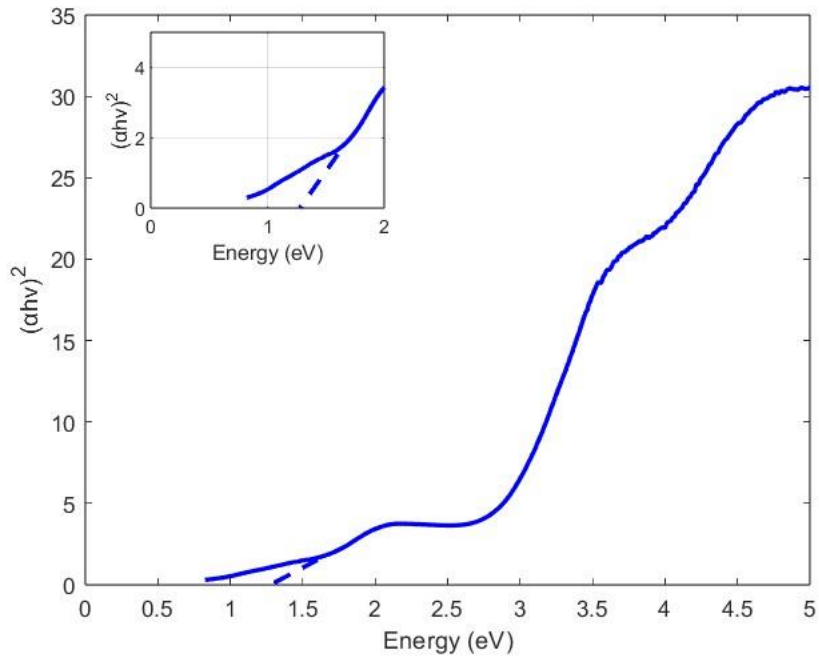


Figure S5. Tauc plot for $\text{Zn}_3(\text{HOTP})_2$ in the coordinates for direct allowed transitions. The inset shows a zoomed-in view of the fitted region, with the best-fit line shown in dotted blue. The extrapolated onset indicates a direct band gap of approximately **~1.3 eV**, which agrees with the onset observed in the UV-Vis spectrum and is consistent with a ligand-centered transition.

7. Crystallographic Table

Table S1. Crystallographic information

Experimentation information	
instrument	Philips Tecnai G2 20
radiation type	Electrons
wavelength (Å)	0.02508
collection method	Continuous rotation
tilt range and step (α_{\min} , α_{\max} , $\Delta\alpha$ (deg.))	-55, 55, 0.3
exposure time (ms)	799
beam diameter (nm)	1000
temperature (K)	298
crystal size (nm)	250x250x500
apparent mosaicity (deg.)	0.18
Structure information	
trivial name	Zn ₃ HOTP ₂
sum formula	Zn C ₁₂ O ₄ H ₄
Z, Z'	3, 1
superspace group	P6 ₃ /mmc(00γ)00ss
a, b, c (Å), V (Å ³)	20.866(9), 20.866(9), 3.1649(5), 1193.4(8)
modulation vector	(0, 0, 0.3488)
completeness (%)	92.5
sin(θ_{\max})/λ (Å ⁻¹)	0.6
N _{obs} (main, satellites, all)	279, 218, 497
N _{all} (main, satellites, all)	455, 638, 1093
Refined parameters	64
R(obs) (I>3σ; %, main refl, satellites, all)	19.45, 21.25, 19.92
R(all) (%), main refl, satellites, all)	24.24, 40.13, 29.04
wR(all) (%), main refl, satellites, all)	22.23, 26.26, 23.92
GoF	3.09

8. Reciprocal space sections

The reciprocal space sections below were calculated with applied lattice symmetry.

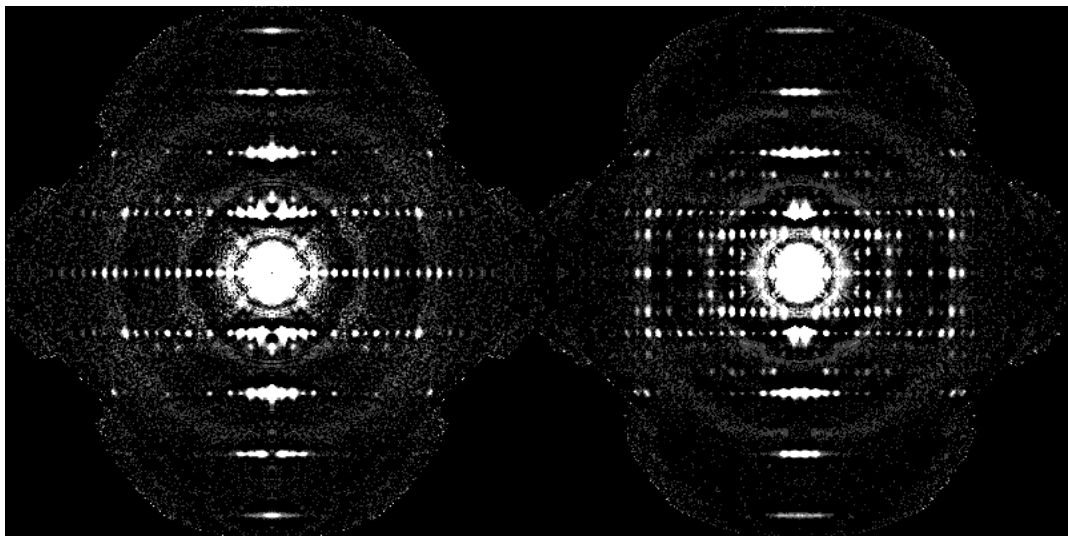


Figure S6. Synthesized precession images for $(0kl)$ and $(1kl)$.

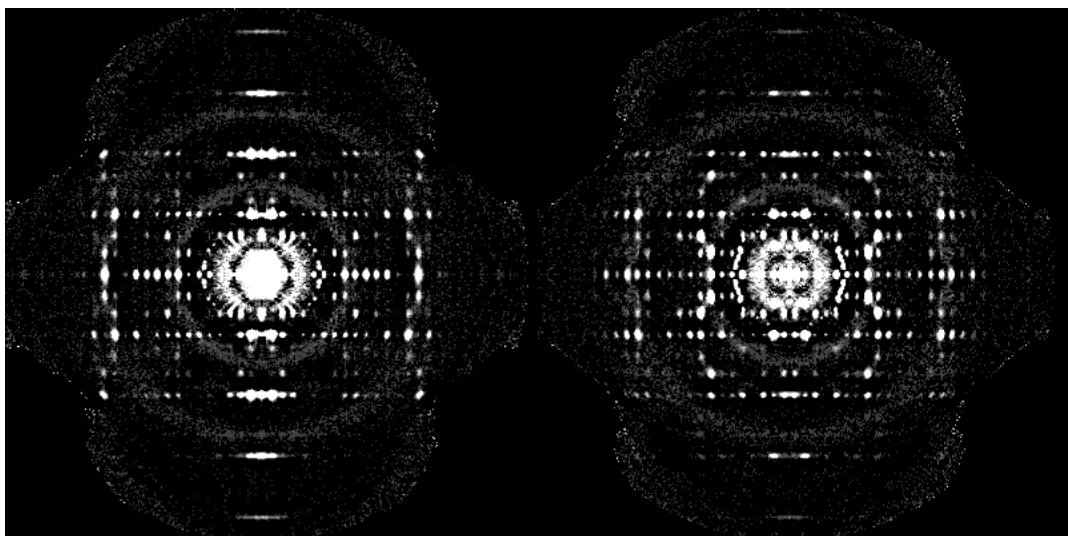


Figure S7. Synthesized precession images for $(2kl)$ and $(3kl)$.

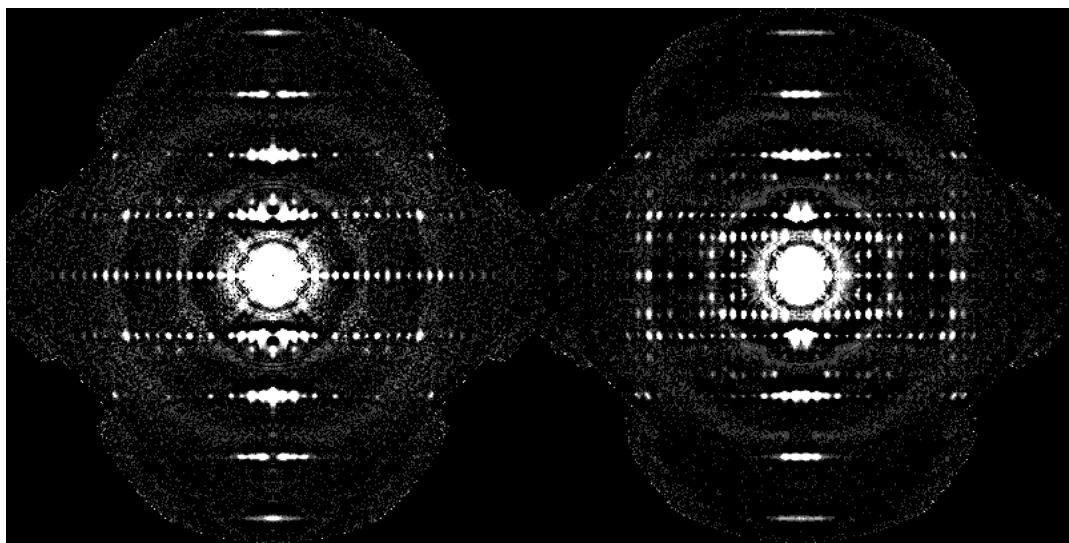


Figure S8. Synthesized precession images for $(h0l)$ and $(h1l)$.

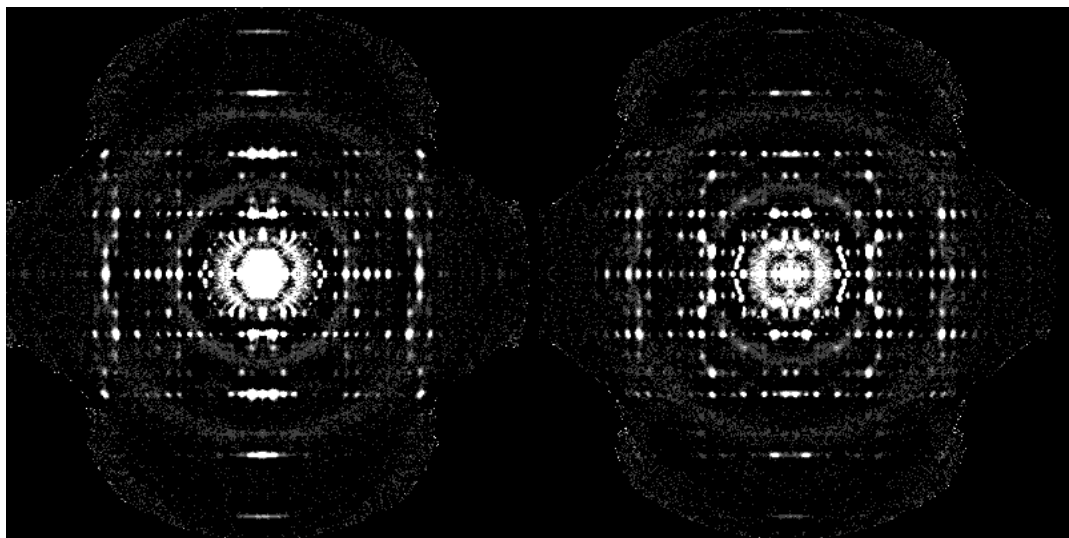


Figure S9. Synthesized precession images for $(h2l)$ and $(h3l)$.

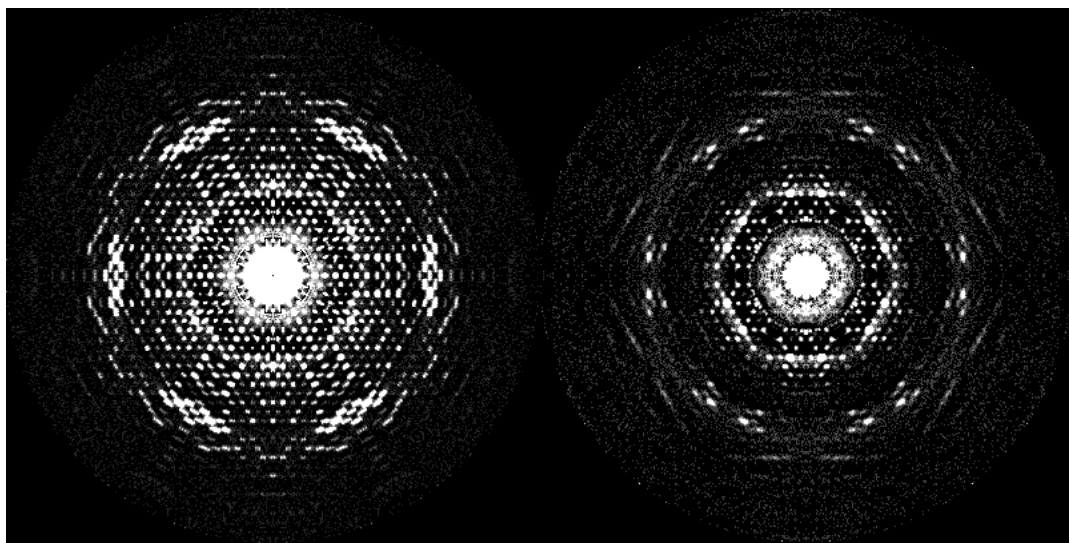


Figure S10. Synthesized precession images for $(hk0)$ and (hkq) .

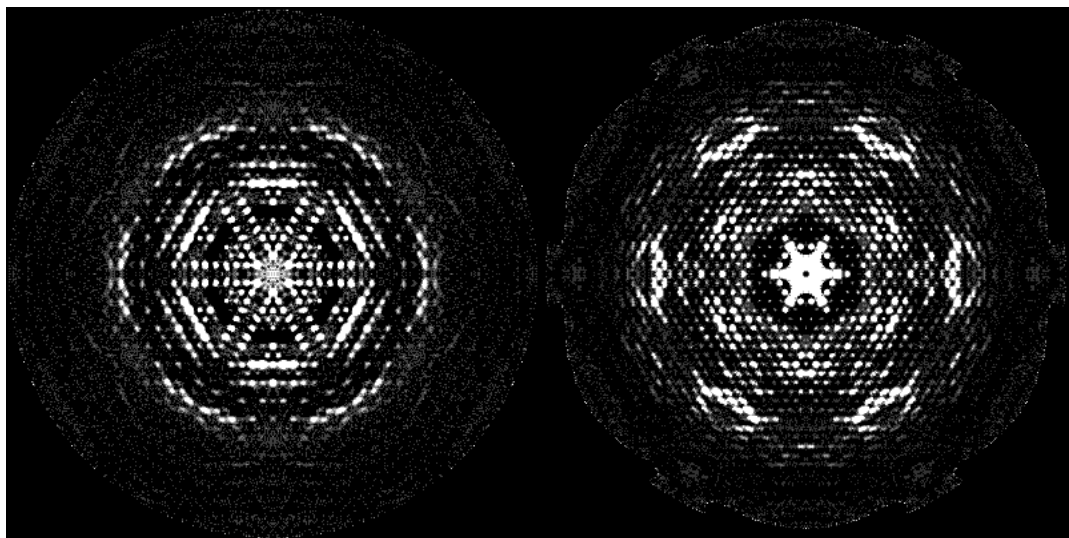


Figure S11. Synthesized precession images for $(hk1-q)$ and $(hk1)$.

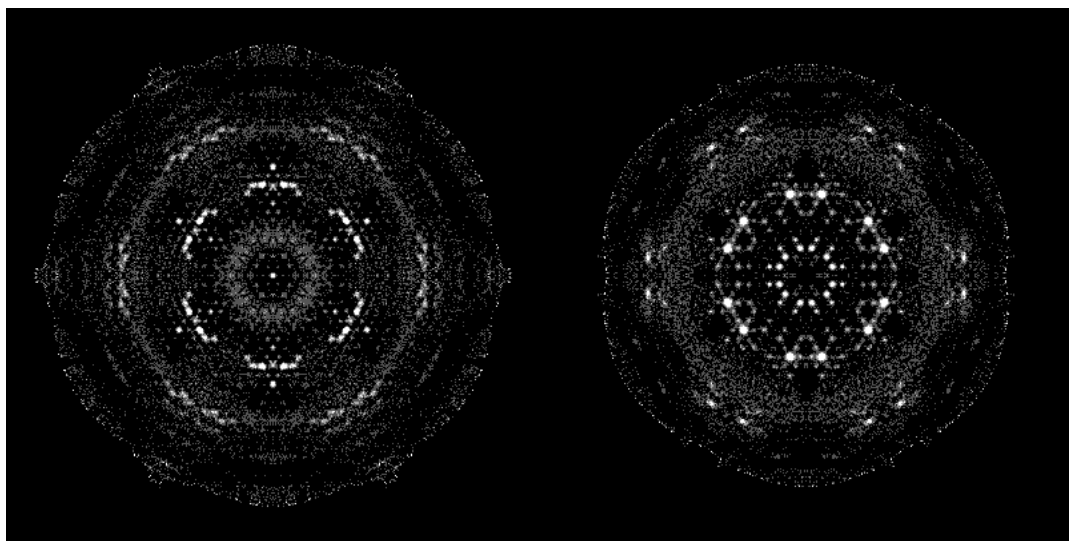


Figure S12. Synthesized precession images for $(hk1+q)$ and $(hk2-q)$.

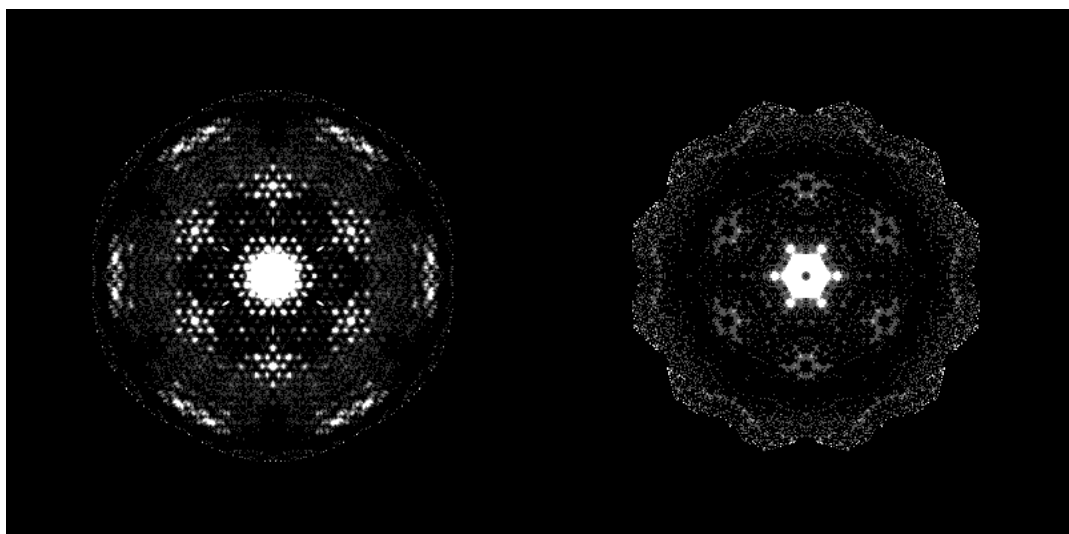


Figure S13. Synthesized precession images for $(hk2)$ and $(hk3)$.

The reciprocal space sections below were calculated without applied lattice symmetry.

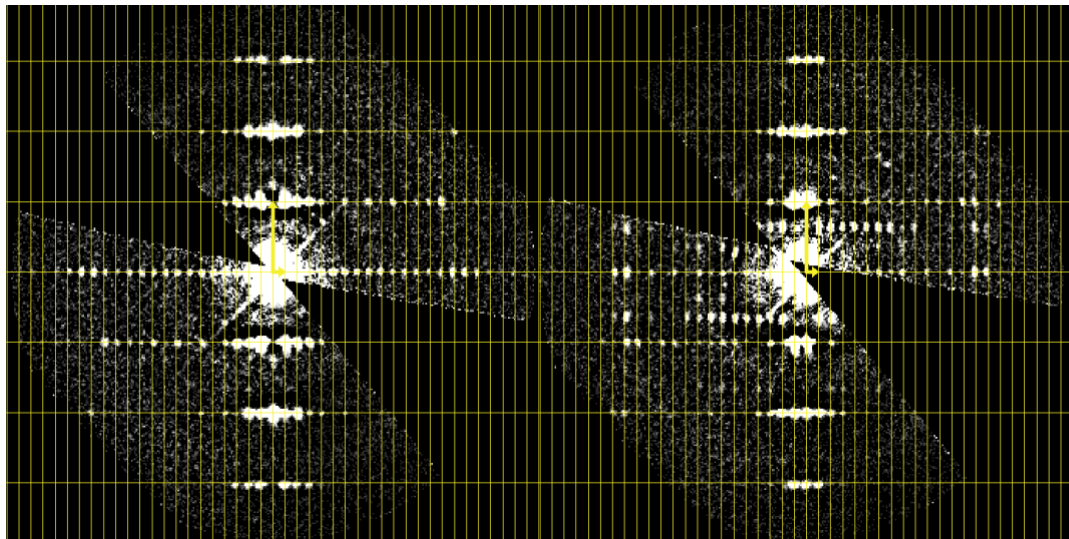


Figure S14. Synthesized precession images for $(0kl)$ and $(1kl)$.

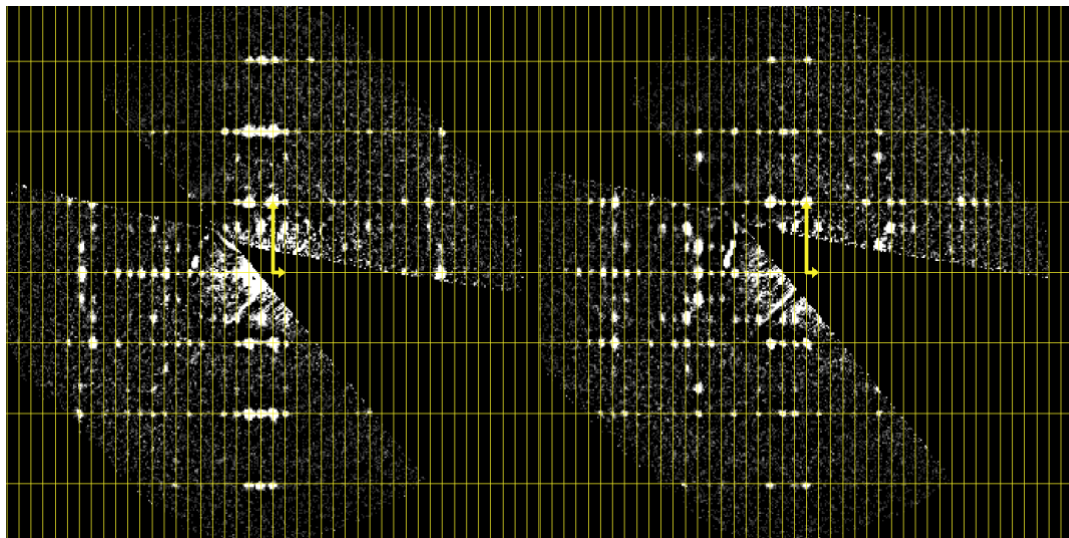


Figure S15. Synthesized precession images for $(2kl)$ and $(3kl)$.

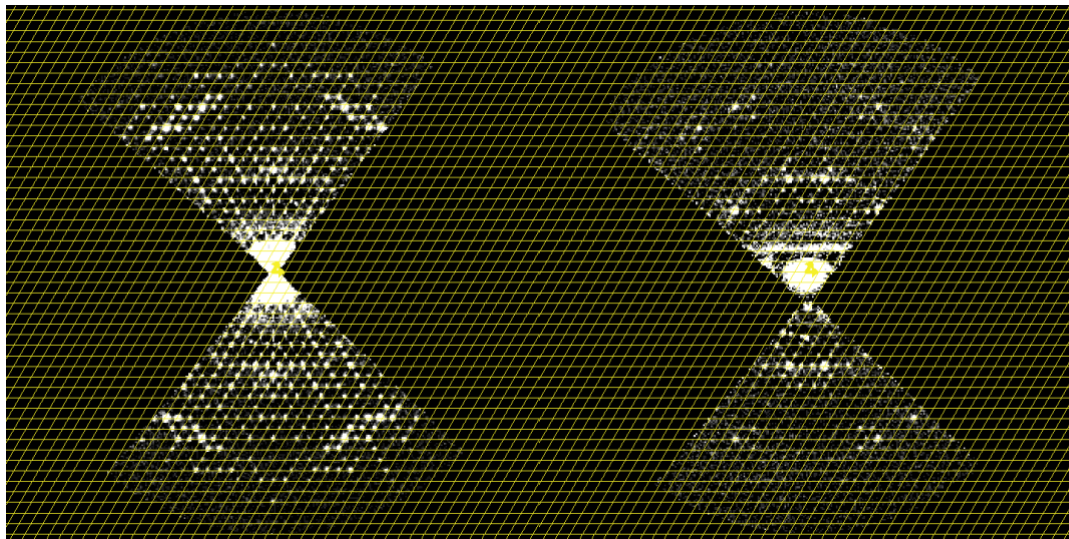


Figure S16. Synthesized precession images for $(hk0)$ and (hkq) .

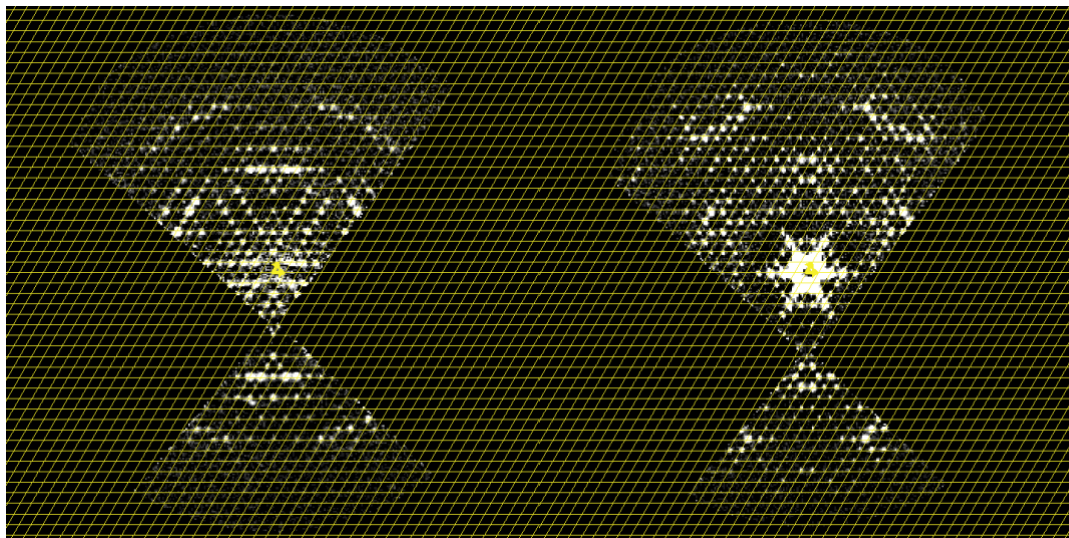


Figure S17. Synthesized precession images for $(hk1-q)$ and $(hk1)$.

9. DFT Optimized Structure

Table S2: DFT optimized structure starting from the 3-fold commensurate

lattice_vector	20.86619900	0.00000000	0.00000000
lattice_vector	-10.43309950	18.07065841	0.00000000
lattice_vector	0.00000000	0.00000000	9.49480000

atom_frac	0.00553325	0.54747920	0.25000023 Zn
atom_frac	0.45226443	0.45783045	0.24999993 Zn
atom_frac	0.54216752	0.99425772	0.24999982 Zn
atom_frac	0.36438324	0.44544826	0.75000002 O
atom_frac	0.55529652	0.91954759	0.74999973 O
atom_frac	0.08107439	0.63627313	0.75000017 O
atom_frac	0.91820524	0.55635167	0.25000024 O
atom_frac	0.44337584	0.36159301	0.24999995 O
atom_frac	0.63829985	0.08160387	0.24999980 O
atom_frac	0.50600999	0.56594312	0.74999993 O
atom_frac	0.43469049	0.94060999	0.74999973 O
atom_frac	0.05999489	0.49460104	0.75000027 O
atom_frac	0.93897578	0.43887751	0.25000011 O
atom_frac	0.56085704	0.49978293	0.24999998 O
atom_frac	0.50003300	0.06076712	0.24999994 O
atom_frac	0.37289194	0.50770754	0.75000002 C
atom_frac	0.49303465	0.86580850	0.74999979 C
atom_frac	0.13483395	0.62778267	0.75000015 C
atom_frac	0.86142682	0.49156292	0.25000017 C
atom_frac	0.50813963	0.36953884	0.24999999 C
atom_frac	0.63024993	0.13836594	0.24999989 C
atom_frac	0.31233179	0.52251261	0.75000008 C
atom_frac	0.47820568	0.79043455	0.74999987 C
atom_frac	0.21021109	0.68838044	0.75000004 C
atom_frac	0.78924670	0.47853924	0.25000014 C
atom_frac	0.52114208	0.31035560	0.25000001 C
atom_frac	0.68938058	0.21054296	0.24999993 C
atom_frac	0.32193594	0.59242539	0.75000005 C
atom_frac	0.40827173	0.73013492	0.74999992 C
atom_frac	0.27051311	0.67874195	0.75000001 C
atom_frac	0.72900770	0.40730246	0.25000007 C
atom_frac	0.59240821	0.32139733	0.25000002 C
atom_frac	0.67833187	0.27074899	0.24999999 C
atom_frac	0.39628181	0.65567332	0.74999996 C
atom_frac	0.34500848	0.74120343	0.74999992 C
atom_frac	0.25944259	0.60440759	0.75000010 C
atom_frac	0.74040302	0.34479088	0.25000002 C
atom_frac	0.65494306	0.39530546	0.25000004 C
atom_frac	0.60442784	0.25934708	0.25000002 C
atom_frac	0.45618325	0.64431834	0.74999992 C
atom_frac	0.35638296	0.81245313	0.74999985 C
atom_frac	0.18818655	0.54449910	0.75000020 C
atom_frac	0.81166163	0.35633690	0.25000002 C
atom_frac	0.64338029	0.45500498	0.25000005 C
atom_frac	0.54474608	0.18806533	0.25000002 C

atom_frac	0.44875075	0.57445295	0.74999995 C
atom_frac	0.42625545	0.87489466	0.74999978 C
atom_frac	0.12574413	0.55190971	0.75000022 C
atom_frac	0.87298870	0.42713358	0.25000009 C
atom_frac	0.57258716	0.44553032	0.25000001 C
atom_frac	0.55425637	0.12677111	0.24999996 C
atom_frac	0.25826210	0.47353449	0.75000015 H
atom_frac	0.52717197	0.78532310	0.74999988 H
atom_frac	0.21530632	0.74245109	0.74999996 H
atom_frac	0.78304409	0.52682597	0.25000018 H
atom_frac	0.47286948	0.25586040	0.25000000 H
atom_frac	0.74387938	0.21677519	0.24999989 H
atom_frac	0.51234394	0.68995630	0.74999986 H
atom_frac	0.31075630	0.82299451	0.74999986 H
atom_frac	0.17768665	0.48834645	0.75000026 H
atom_frac	0.82355153	0.31165883	0.24999998 H
atom_frac	0.68806253	0.51157387	0.25000007 H
atom_frac	0.48816967	0.17615529	0.25000004 H
atom_frac	0.54306187	0.55045622	0.55518607 Zn
atom_frac	0.44946694	0.99265727	0.55458358 Zn
atom_frac	0.00742557	0.45689326	0.55542395 Zn
atom_frac	0.54306186	0.55045624	0.94481383 Zn
atom_frac	0.44946697	0.99265728	0.94541579 Zn
atom_frac	0.00742557	0.45689329	0.94457663 Zn
atom_frac	0.64119163	0.55757143	0.57171839 O
atom_frac	0.44231650	0.08360797	0.57154860 O
atom_frac	0.91639047	0.35873396	0.57208626 O
atom_frac	0.64119162	0.55757145	0.92828150 O
atom_frac	0.44231652	0.08360800	0.92845106 O
atom_frac	0.91639049	0.35873401	0.92791417 O
atom_frac	0.08447870	0.44515204	0.46498567 O
atom_frac	0.55478006	0.63925157	0.46475194 O
atom_frac	0.36062510	0.91542438	0.46481094 O
atom_frac	0.08447869	0.44515210	0.03501499 O
atom_frac	0.55478007	0.63925163	0.03524785 O
atom_frac	0.36062514	0.91542444	0.03518855 O
atom_frac	0.50410393	0.44247315	0.57503189 O
atom_frac	0.55743668	0.06161977	0.57445865 O
atom_frac	0.93831166	0.49577077	0.57491489 O
atom_frac	0.50410392	0.44247317	0.92496815 O
atom_frac	0.55743671	0.06161983	0.92554071 O
atom_frac	0.93831166	0.49577081	0.92508559 O
atom_frac	0.06080059	0.55758196	0.42072348 O
atom_frac	0.44229192	0.50311312	0.42070428 O
atom_frac	0.49675741	0.93908599	0.42066943 O
atom_frac	0.06080062	0.55758206	0.07927697 O
atom_frac	0.44229194	0.50311319	0.07929569 O
atom_frac	0.49675745	0.93908608	0.07933009 O
atom_frac	0.63321820	0.49366827	0.57434325 C
atom_frac	0.50622910	0.13953394	0.57421801 C
atom_frac	0.86042133	0.36665212	0.57448098 C
atom_frac	0.63321819	0.49366829	0.92565673 C
atom_frac	0.50622911	0.13953398	0.92578171 C

atom_frac	0.86042135	0.36665216	0.92551934 C
atom_frac	0.14000160	0.50802736	0.43645914 C
atom_frac	0.49187798	0.63188583	0.43646093 C
atom_frac	0.36799782	0.85989192	0.43646225 C
atom_frac	0.14000161	0.50802744	0.06354134 C
atom_frac	0.49187799	0.63188589	0.06353893 C
atom_frac	0.36799786	0.85989200	0.06353737 C
atom_frac	0.69183227	0.47941733	0.57645138 C
atom_frac	0.52048540	0.21239033	0.57645989 C
atom_frac	0.78755129	0.30802245	0.57654098 C
atom_frac	0.69183227	0.47941735	0.92354864 C
atom_frac	0.52048540	0.21239036	0.92354006 C
atom_frac	0.78755131	0.30802250	0.92345919 C
atom_frac	0.21197783	0.52098807	0.42386127 C
atom_frac	0.47889203	0.69089422	0.42408270 C
atom_frac	0.30898138	0.78791490	0.42399090 C
atom_frac	0.21197785	0.52098815	0.07613912 C
atom_frac	0.47889205	0.69089430	0.07591711 C
atom_frac	0.30898141	0.78791499	0.07600888 C
atom_frac	0.67956303	0.40810274	0.57739985 C
atom_frac	0.59180992	0.27141899	0.57741974 C
atom_frac	0.72852210	0.32033386	0.57741937 C
atom_frac	0.67956303	0.40810277	0.92260021 C
atom_frac	0.59180993	0.27141903	0.92258024 C
atom_frac	0.72852212	0.32033390	0.92258068 C
atom_frac	0.27146795	0.59228424	0.41399683 C
atom_frac	0.40760941	0.67910197	0.41411051 C
atom_frac	0.32078810	0.72842789	0.41404703 C
atom_frac	0.27146797	0.59228432	0.08600336 C
atom_frac	0.40760944	0.67910205	0.08588939 C
atom_frac	0.32078813	0.72842798	0.08595284 C
atom_frac	0.60470787	0.34575475	0.57750580 C
atom_frac	0.65416373	0.25891349	0.57745090 C
atom_frac	0.74100444	0.39518326	0.57741497 C
atom_frac	0.60470788	0.34575478	0.92249428 C
atom_frac	0.65416375	0.25891354	0.92254898 C
atom_frac	0.74100445	0.39518330	0.92258513 C
atom_frac	0.25965608	0.65438279	0.41217218 C
atom_frac	0.34551366	0.60519733	0.41224343 C
atom_frac	0.39469626	0.74023873	0.41225267 C
atom_frac	0.25965611	0.65438288	0.08782786 C
atom_frac	0.34551369	0.60519741	0.08775667 C
atom_frac	0.39469629	0.74023881	0.08774715 C
atom_frac	0.54587005	0.35795398	0.57813672 C
atom_frac	0.64193656	0.18787495	0.57792376 C
atom_frac	0.81204003	0.45400503	0.57786406 C
atom_frac	0.54587005	0.35795401	0.92186341 C
atom_frac	0.64193658	0.18787501	0.92207593 C
atom_frac	0.81204003	0.45400507	0.92213615 C
atom_frac	0.18804748	0.64196408	0.41229736 C
atom_frac	0.35793737	0.54601074	0.41249561 C
atom_frac	0.45388530	0.81184278	0.41244051 C
atom_frac	0.18804751	0.64196418	0.08770274 C

atom_frac	0.35793740	0.54601082	0.08750455 C
atom_frac	0.45388534	0.81184286	0.08755920 C
atom_frac	0.55654719	0.42955041	0.57590073 C
atom_frac	0.57034342	0.12697355	0.57559100 C
atom_frac	0.87295299	0.44331985	0.57579507 C
atom_frac	0.55654718	0.42955044	0.92409933 C
atom_frac	0.57034344	0.12697360	0.92440857 C
atom_frac	0.87295300	0.44331989	0.92420527 C
atom_frac	0.12857834	0.57132563	0.41950151 C
atom_frac	0.42857362	0.55716442	0.41955381 C
atom_frac	0.44271848	0.87131261	0.41953346 C
atom_frac	0.12857837	0.57132572	0.08049883 C
atom_frac	0.42857364	0.55716449	0.08044620 C
atom_frac	0.44271852	0.87131269	0.08046615 C
atom_frac	0.74659512	0.52722521	0.57603805 H
atom_frac	0.47268891	0.21936037	0.57609106 H
atom_frac	0.78057894	0.25325492	0.57623714 H
atom_frac	0.74659511	0.52722524	0.92396195 H
atom_frac	0.47268891	0.21936040	0.92390899 H
atom_frac	0.78057897	0.25325497	0.92376301 H
atom_frac	0.21873303	0.47318518	0.43220641 H
atom_frac	0.52669344	0.74545141	0.43249643 H
atom_frac	0.25442613	0.78116550	0.43235271 H
atom_frac	0.21873304	0.47318524	0.06779408 H
atom_frac	0.52669346	0.74545148	0.06750324 H
atom_frac	0.25442617	0.78116558	0.06764710 H
atom_frac	0.48903618	0.31398830	0.57993860 H
atom_frac	0.68589344	0.17499230	0.57962919 H
atom_frac	0.82491504	0.51084388	0.57952953 H
atom_frac	0.48903618	0.31398833	0.92006159 H
atom_frac	0.68589347	0.17499235	0.92037042 H
atom_frac	0.82491505	0.51084391	0.92047072 H
atom_frac	0.17574459	0.68631792	0.40686117 H
atom_frac	0.31358494	0.48935154	0.40714847 H
atom_frac	0.51054158	0.82414260	0.40702451 H
atom_frac	0.17574463	0.68631802	0.09313881 H
atom_frac	0.31358498	0.48935163	0.09285181 H
atom_frac	0.51054162	0.82414268	0.09297517 H

10. Room temperature conductivity measurements

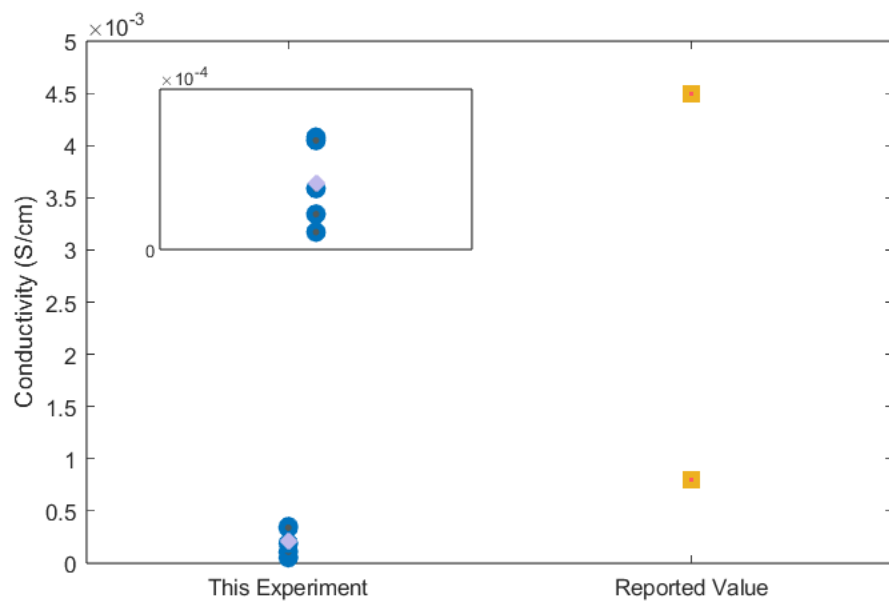


Figure S18. Two-contact probe room temperature conductivity measurement. Blue: electrical conductivity of six different batches of $\text{Zn}_3(\text{HOTP})_2$, purple: average measured conductivity, yellow: reported value of electrical conductivity of $\text{Zn}_3(\text{HOTP})_2$.^{9,10}

11. References

1. Blum V, Gehrke R, Hanke F, Havu P, Havu V, Ren X, et al. Ab initio molecular simulations with numeric atom-centered orbitals. *Comput Phys Commun.* 2009 Nov;180(11):2175–96.
2. Perdew JP, Burke K, Ernzerhof M. Generalized Gradient Approximation Made Simple. 1996.
3. Paier J, Marsman M, Hummer K, Kresse G, Gerber IC, Angyán JG. Erratum: Screened hybrid density functionals applied to solids (*Journal of Chemical Physics* (2006) 124 (154709)). Vol. 125, *Journal of Chemical Physics*. 2006.
4. Monkhorst HJ, Pack JD. Special points for Brillouin-zone integrations*. Vol. 13, NUMBER. 1976.
5. Palatinus L, Brázda P, Jel\'inek M, Hrdá J, Steciuk G, Klementová M. Specifics of the data processing of precession electron diffraction tomography data and their implementation in the program PETS2.0. *Acta Crystallographica Section B [Internet]*. 2019 Aug;75(4):512–22. Available from: <https://doi.org/10.1107/S2052520619007534>
6. Petříček V, Palatinus L, Plášil J, Dušek M. Jana 2020 - a new version of the crystallographic computing system Jana. *Z Kristallogr Cryst Mater.* 2023 Jul 1;238(7–8):271–82.
7. Palatinus L, Chapuis G. SUPERFLIP – a computer program for the solution of crystal structures by charge flipping in arbitrary dimensions. *J Appl Crystallogr [Internet]*. 2007 Aug;40(4):786–90. Available from: <https://doi.org/10.1107/S0021889807029238>
8. Palatinus L. Ab initio determination of incommensurately modulated structures by charge flipping in superspace. *Acta Crystallographica Section A [Internet]*. 2004 Nov;60(6):604–10. Available from: <https://doi.org/10.1107/S0108767304022433>
9. Chen Y, Zhu Q, Fan K, Gu Y, Sun M, Li Z, et al. Successive Storage of Cations and Anions by Ligands of π-d-Conjugated Coordination Polymers Enabling Robust Sodium-Ion Batteries. *Angewandte Chemie - International Edition*. 2021 Aug 16;60(34):18769–76.
10. Choi JY, Stodolka M, Kim N, Pham HTB, Check B, Park J. 2D conjugated metal-organic framework as a proton-electron dual conductor. *Chem.* 2023 Jan 12;9(1):143–53.